Watersheds on the Cortical Surface for Automated Sulcal Segmentation

Maryam E. Rettmann*, Xiao Han†, and Jerry L. Prince†*
*Department of Biomedical Engineering
†Department of Electrical and Computer Engineering
Center for Imaging Science
The Johns Hopkins University, Baltimore, MD 21218
prince@jhu.edu

Abstract

The human cortical surface is a highly complex, folded structure. Cortical sulci, the spaces between the folds, define location on the cortex and provide a parcellation into functionally distinct areas. A topic that has recently received increased attention is the segmentation of these sulci from magnetic resonance (MR) images, with most work focussing on the extraction of the sulcal spaces between the folds. Unlike these methods, we propose a technique that extracts actual regions of the cortical surface that surround sulci which we call "sulcal regions". The method is based on a watershed algorithm applied to a geodesic distance transform on the cortical surface. A well known problem with the watershed algorithm is a tendency towards oversegmentation. To address this problem, we propose a post-processing algorithm that merges appropriate segments from the watershed algorithm.

1. Introduction

Quantitative anatomic studies of the human cortex are challenging due to its highly complex, convoluted folding pattern. Ridges of the folds, called gyri, and the spaces between the folds, called sulci, define location on the cortical surface and provide a parcellation of the cortex into functionally distinct areas. With the advancement of magnetic resonance (MR) imaging techniques, high-resolution, high contrast three-dimensional images of the brain can now be routinely acquired in vivo. As a result, methods for modelling the cortical surface from these images have emerged, providing a means for furthering the understanding of morphometric variability in human populations. A topic that has recently received increased attention is the study of sulci, in particular, their segmentation from MR images [14, 15, 4, 9, 6, 7, 19]. Sulci segmented from the cortex can be used in a variety of applications such as deformable atlas registration algorithms and localizing activation sites in functional imaging. In addition, the geometric analysis of sulci will lead to a better understanding of normal versus diseased cortical geometry and the morphological changes that occur with disease.

Previous work in the segmentation of sulci has focussed on either fitting a surface [14, 15, 4, 19], finding a set of points [9] or extracting the volumetric regions [6, 7] within the sulcal spaces. Unlike these methods, we propose a technique that segments the actual cortical regions surrounding sulci. The advantage of segmenting actual cortical regions is that it allows for a direct geometric study of the cortical surface and provides a means for mapping functional activation sites. For ease of terminology, we refer to our segmented regions as "sulcal regions", meaning precisely the buried regions of cortex surrounding the sulcal spaces. Another advantage of the proposed method is that it segments sulcal regions on the medial surface as well as the lateral and inferior surfaces. Also, this segmentation method is completely automated except for picking a seed point on the cortical surface.

In this paper, we describe our methodology for automatically segmenting sulcal regions using a watershed algorithm applied to a geodesic distance transform. A well known problem with the watershed algorithm is a tendency towards oversegmentation. To address this problem, we propose a post-processing algorithm that merges appropriate segments from the watershed algorithm. The idea of sulcal segmentation using watersheds was first introduced by Lohmann and von Cramon in [6] and extended in [7]. Although our method is similar in basic concept to that described by Lohmann, there are several important distinctions. First, our method operates on a cortical surface mesh extracted from MR images as opposed to Lohmann's

This work was partially supported by the NSF ERC/CISST#9731748 and by the NIH/NINDS R01NS37747 and a Whitaker Foundation graduate fellowship.

0-7695-0737-9/00 $10.00 (c) 2000 IEEE

method that operates directly on the image data. Second, the result of our segmentation is a piece of the cortical surface, defined on the continuum, while volumes corresponding to the gray matter and sulcal spaces are extracted in the work of Lohmann. The relationship between the two results is that our surface segments pass through the volumes extracted by Lohmann. Finally, our method segments sulci from the lateral, medial and inferior surfaces of the brain while the work in [6, 7] focuses on sulci from the lateral surface only.

This paper is an extension of our previous work on sulcal segmentation [11] offering several important improvements. First, the geodesic distance transform is used as opposed to the Euclidean distance transform. Second, the previous method required an initial depth threshold value to begin the segmentation. In this method, the segmentation begins at the deepest cortical regions eliminating the need for a user defined initial value. Finally, in this method, the watershed algorithm produces segments that completely parcellate the sulcal regions.

2. Problem description

The goal of this segmentation work is to extract the buried cortical regions surrounding each of the sulcal spaces. These regions, which we term "sulcal regions", are depicted in Fig. 1 on a simplified illustration of the cortex. As illustrated in the figure, sulcal regions are separated by a ridge.

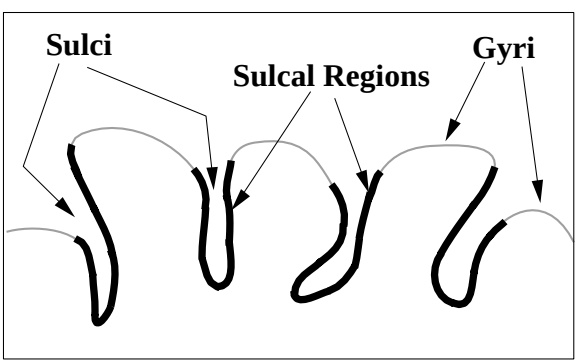

Figure 1. A simplified illustration of a cross-section of the cortical surface.

For illustration purposes, a three-dimensional diagram representing two sulcal regions is shown in Fig. 2(a). The ideal segmentation, according to our definition of sulcal regions, is shown in Fig. 2(b) where one of the sulcal regions is outlined in light gray line and the other in dark gray. This diagram demonstrates that the ideal segmentation is identical to the result that would be obtained by applying a three-dimensional watershed algorithm to the surface depicted in Fig. 2(a).

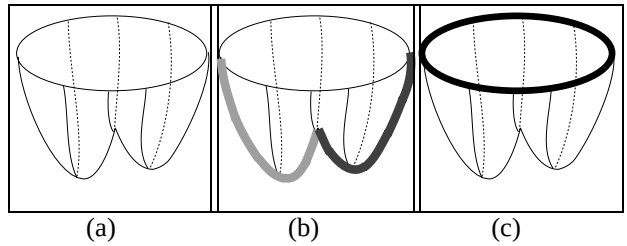

Figure 2. A simplified illustration of (a) two sulcal regions, (b) their ideal segmentation and (c) a gyral region.

Traditionally, the watershed algorithm has been used in image processing for segmenting images into various catchment basins or extracting watershed lines. We employ the same concepts of this algorithm to segment sulcal regions from a cortical surface mesh. While a complete description of the watershed algorithm can be found in [16], the key ideas are illustrated in Fig. 3. As depicted on the left, the watershed algorithm can be viewed as puncturing holes at the local minima of a function and beginning to fill these regions with water. Each region filling with water is called a catchment basin. When the water from two catchment basins begins to merge, a dam is constructed to prevent water from one catchment basin from spilling into the other. These dams are termed watershed lines.

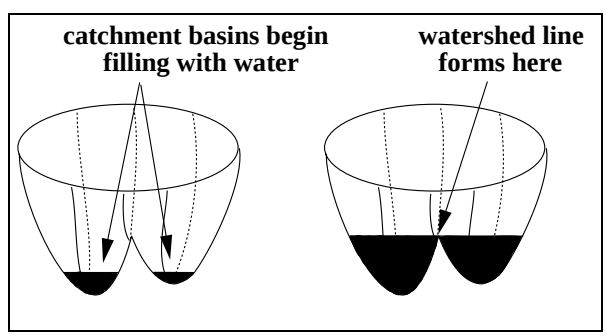

Figure 3. Illustration of watershed algorithm.

From the above illustrations, it is clear that the watershed computed on a function that describes the cortical convolutions would provide an appropriate segmentation of sulcal regions. The challenge in employing the watershed lies in defining this function. We have chosen to model the cortical convolutions by computing a function based on the depth of

0-7695-0737-9/00 $10.00 (c) 2000 IEEE

each point in the sulcal regions with respect to the gyral regions. This depth function is generated in the following manner. First, the cortical surface is parcellated into gyral and sulcal regions. In the simplified example, the gyral region corresponds to the dark colored ridge in Fig. 2(c). Next, the geodesic distance transform from the sulcal regions to the gyral regions is computed. Geodesic distance is defined as the length of the shortest path along the cortical surface between two points. Thus, the transform assigns to each point in a sulcal region, the length of the shortest path to a gyral region. This results in points at the bottom of a sulcal region having large values and points close to gyri having small values. A simple remapping of the depth values such that large depths correspond to small values and vice versa results in a two-dimensional function that describes the cortical convolutions.

A typical problem encountered with the watershed algorithm is its tendency towards oversegmentation [16]. A single region will be segmented as several catchment basins due to noise or small variations in the function. In our application, this corresponds to several catchment basins forming as a result of small ridges in the sulcal regions. To address this issue, we propose a post-processing algorithm to merge catchment basins based on the height of the ridge separating them.

3. Initial data and model

Although our method is generally applicable to any reconstructed cortical surface [1, 8, 3, 2, 12, 17], in this work, we use surfaces reconstructed from MR images using the technique described in [18]. This technique combines fuzzy segmentation, isosurfaces and deformable surface models to reconstruct the layer of cortex lying in the geometric center, which is approximately cytoarchitectonic layer 4. The reconstruction method is composed of three major steps. First, a three-class fuzzy segmentation of the MR data is computed corresponding to gray matter, white matter and cerebrospinal fluid. Second, an initialization for the deformable surface model is created by generating a smoothed isosurface from the white matter membership function obtained from the segmentation. The result of the isosurface algorithm is a mesh that is a discrete representation of the continuous isosurface. Finally, a deformable surface model is used to refine the initial surface to the central layer of the gray matter. The cortex reconstruction method requires a minimal amount of manual interaction and is capable of fully resolving deep convoluted folds. The resulting surface is represented by a triangular mesh consisting of approximately 300,000 vertices.

To allow visualization of buried cortical regions, a spherical representation of the reconstructed cortical surface is generated that maintains a one-to-one mapping with the original reconstructed surface. The spherical map generation is described in [11] and is used to aid in visualization of both functions on the cortical surface and the final segmented sulcal regions.

4. Segmentation method

In this section, we present the steps required to generate a function that describes the cortical convolutions. The results of the watershed applied to this function are demonstrated, followed by a description of the catchment basin merging algorithm.

4.1. Parcellation into gyral and sulcal regions

First, the cortical surface is parcellated into the outer, gyral regions and the buried, sulcal regions. Gyral regions are distinguishable from sulcal regions in that they lie on the outer surface of the cortex. This outer cortical surface can be represented by a "shrink-wrap" surface that tightly surrounds the cortical surface but does not enter into the cortical folds. In order to parcellate sulcal regions on the medial surfaces as well as the lateral and inferior surfaces, a shrink-wrap surface must be generated for each hemisphere separately. Let $\mathcal{B}_j$ be the set of all vertices on the shrink-wrap surface corresponding to the jth hemisphere where $j \in \{1, 2\}$. Fig. 4 is a coronal cross-section showing a contour of a shrink-wrap surface in gray and the reconstructed cortical surface in white. A detailed description of the shrink-wrap generation can be found in [11].

Figure 4. Cross section of a shrink-wrap surface superimposed on the original cortical surface.

Each vertex on the cortical surface mesh can then be labeled as either gyral or sulcal based on its distance to the appropriate shrink-wrap. This requires each vertex to be labeled according to hemisphere. Let $\mathcal{A}$ be the set of all vertices on the cortical surface mesh. Each vertex $a_i \in \mathcal{A}$

0-7695-0737-9/00 $10.00 (c) 2000 IEEE

is assigned a label indicating which cortical hemisphere it belongs to. Let $l(a_i)$ be the hemisphere label of vertex a_i such that

$$l(a_i) = \begin{cases} 1 & \text{if vertex } a_i \text{ is on hemisphere 1} \\ 2 & \text{if vertex } a_i \text{ is on hemisphere 2} \end{cases} \quad (1)$$

The labels are determined by making a cut through the corpus callosum, separating the cortical surface into two hemispheres. This step requires the user to pick a point in the center of the corpus callosum, the only manual interaction required in the segmentation procedure.

Next, the Euclidean distance transform from the cortical surface to the shrink wrap surfaces is computed. Let

$$D_e(a_i, \mathcal{B}) = \min_{b_j \in \mathcal{B}} \{d_e(a_i, b_j)\} \quad (2)$$

denote the distance from vertex a_i to the nearest vertex $b \in \mathcal{B}$. The function $d_e(a_i, b_j)$ denotes the standard Euclidean distance from vertex a_i to vertex b_j. Then, $e(a_i)$ defined as

$$e(a_i) = \begin{cases} D_e(a_i, \mathcal{B}_1) & \text{if } l(a_i) = 1 \\ D_e(a_i, \mathcal{B}_2) & \text{if } l(a_i) = 2 \end{cases} \quad (3)$$

is the Euclidean distance from a_i to the nearest vertex on its corresponding shrink-wrap surface. The function e is shown on the spherical map in Fig. 5(b) where small distances are shown as light gray and large distances in dark gray. A rendering of the cortical surface is shown in Fig. 5(a) at the same view as the spherical map. The spherical map is rendered with flat shading to avoid confusion with the gray scale distance values.

Finally, the cortical surface can be parcellated into gyral and sulcal regions by assigning labels, $m(a_i)$ to each vertex where

$$m(a_i) = \begin{cases} 1 & \text{if } e(a_i) < \delta \\ 0 & \text{otherwise} \end{cases} \quad (4)$$

A vertex a where $m(a) = 1$ is a gyral vertex, otherwise it is a sulcal vertex. δ was chosen to be two millimeters, meaning that cortical regions within two millimeters of the shrink-wrap are considered gyral. The function m is shown in Fig. 5(c) superimposed on the spherical map where gray areas correspond to sulcal regions.

4.2. Geodesic calculation

Next the geodesic distance transform of vertices in the sulcal regions to the gyral regions is computed. Let $\mathcal{C}$ be the set of all vertices lying on a gyral region of the cortex, which includes all vertices a_i such that $m(a_i) = 1$. Let

$$D_g(a_i, \mathcal{C}) = \min_{c_j \in \mathcal{C}} \{d_g(a_i, c_j)\} \quad (5)$$

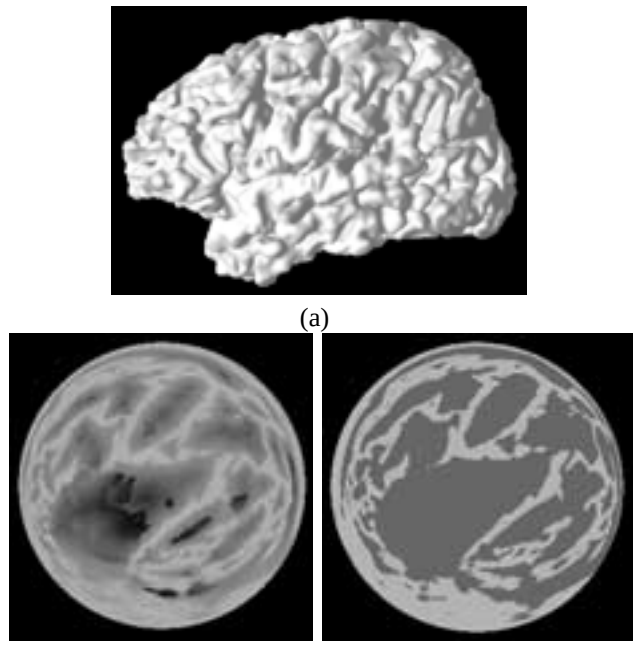

(a) (b) (c)

Figure 5. The Euclidean distance function superimposed on (b) the spherical map which is displayed at the same lateral view as the cortical surface in (a). A thresholding operation applied to the distance function results in (c) a parcellation into gyral and sulcal regions.

define the geodesic distance from vertex a_i to the nearest vertex $c \in \mathcal{C}$. The function $d_g(a_i, c_j)$ denotes geodesic distance from vertex a_i to vertex c_j. Then, $g(a_i)$ defined as

$$g(a_i) = \begin{cases} D_g(a_i, \mathcal{C}) & \text{if } m(a_i) = 0 \\ 0 & \text{if } m(a_i) = 1 \end{cases} \quad (6)$$

is the geodesic distance from a_i to the nearest vertex located on a gyral region and vertices lying in gyral regions are always assigned a distance of zero. The function g is shown in Fig. 6 superimposed on the spherical map where small distances are shown in light gray and large distances in dark gray.

A geodesic distance transform is also employed in [7] where the computation is accomplished using a constrained Euclidean distance measure on the image data. We require a geodesic distance measurement on the surface mesh and have implemented the method proposed by Kimmel and Sethian in [5] for this purpose. In this method, the geodesic distance is computed using a fast marching algorithm for a triangulated mesh. An initial contour is specified at time zero and propagated on the mesh with unit speed in the normal direction. For our application, the initial contour is defined as all vertices lying on the border between gyral and

0-7695-0737-9/00 $10.00 (c) 2000 IEEE

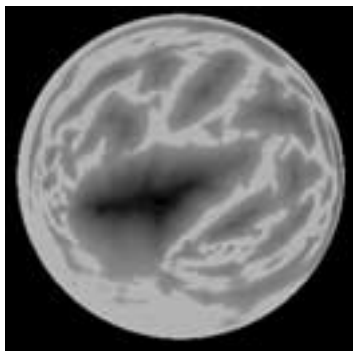

Figure 6. Geodesic distance transform from vertices in sulcal regions to gyral regions.

sulcal regions. The geodesic distance to all other points on the mesh is assigned as the arrival time of the evolving contour.

4.3. Watershed algorithm

The geodesic distance function g is remapped to generate a function on the cortical surface that describes the cortical convolutions in the framework consistent with the watershed algorithm. Define

$$d_{max}(\mathcal{D}, h) = \max_{d_i \in \mathcal{D}} \{h(d_i)\} \tag{7}$$

which is the maximum of h, a function of vertices, over all vertices in the vertex set $\mathcal{D}$. Then

$$f(a_i) = d_{max}(\mathcal{A}, g) - g(a_i) \tag{8}$$

results in the desired remapping.

Next, the watershed of f is computed, resulting in N catchment basins where $\mathcal{J}_i$ is the ith catchment basin comprising a set of vertices. The index i indicates when the catchment basin was formed during the watershed algorithm. The first basin to form is labeled with one, the second with two and so forth. This gives a natural ordering of the deepest to most shallow catchment basins. Vincent describes a fast method for computing the watershed on an image in [16] that generates accurate watershed lines while avoiding thick watershed regions. We used this algorithm for computing the watershed with a few minor adaptations for the mesh.

The result of the watershed applied to the transformed distance map is shown in Fig. 7(a) where the watershed vertices are colored black. This result can be used to generate either the watershed lines or the catchment basins of the sulcal regions by applying different post-processing rules on the watershed vertices. For watershed line extraction, all vertices bordering two catchment basins can be relabeled as watershed vertices. For complete parcellation of the sulcal regions into catchment basins, each watershed vertex is added to its neighboring catchment basin with the smallest numerical label. In this application, the latter rule is applied, with the final watershed result shown in Fig. 7(b). From the figure it is clear that the sulcal regions have been oversegmented, meaning that several catchment basins represent a single sulcal region.

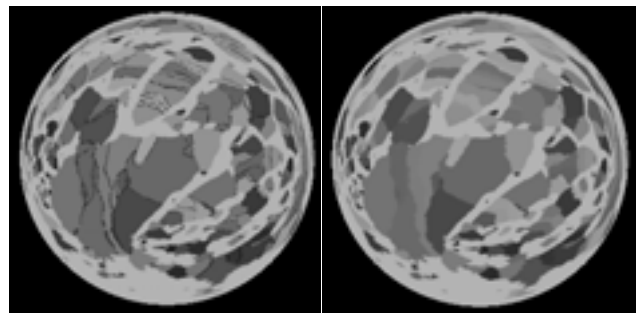

(a) (b)

Figure 7. Result of (a) the watershed algorithm, and (b) the reassignment of watershed vertices to catchment basins.

4.4. Merging of catchment basins

In this step, we address the oversegmentation that has occurred during the watershed transformation. As described previously, small ridges in the sulcal regions will result in the formation of separate catchment basins. The criterion for joining two catchment basins is based on the height of the watershed line separating them. The catchment basins are compared pairwise and basins formed earlier in the watershed algorithm are checked first.

To assist in the joining algorithm, an adjacency graph of the catchment basins is generated where $\mathcal{N}(\mathcal{J}_i)$ is the set of catchment basins adjacent to $\mathcal{J}_i$. The joining algorithm follows:

/⋆generate a list of all catchment basins (CBs) in the order they were formed during the watershed algorithm ⋆/
CBlist $\leftarrow$ *list of* $\mathcal{J}_1 \ldots \mathcal{J}_N$
numMerges $\leftarrow$ *0*
while end of list has not been reached
  $\mathcal{J}$ $\leftarrow$ *next CB on list*
  $\mathcal{K}$ $\leftarrow$ *CB in set* $\mathcal{N}(\mathcal{J})$ *with smallest numerical label*
  $\mathcal{E}$ $\leftarrow$ *set of vertices on border between* $\mathcal{J}$ *and* $\mathcal{K}$
  if $(d_{max}(\mathcal{E}, g) - d_{max}(\mathcal{J}, g) < \delta)$ *AND*
    $(d_{max}(\mathcal{E}, g) - d_{max}(\mathcal{K}, g) < \delta)$
    merge $\mathcal{K}$ *to* $\mathcal{J}$

0-7695-0737-9/00 $10.00 (c) 2000 IEEE

remove $\mathcal{K}$ from CBlist
$\mathcal{J}$ inherits $\mathcal{N}(\mathcal{K})$ except duplicates
numMerges ← numMerges+1
end if
end while
if (numMerges = 0)
quit
else
numMerges ← 0
repeat while loop starting at beginning of list

The merging criterion is depicted in Fig. 8 and is similar in concept to that proposed in [7]. If the relative height of the watershed line separating two catchment basins is small, these basins are merged.

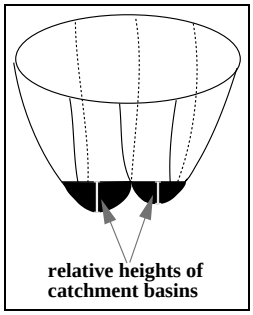

Figure 8. Illustration of merging criterion.

An example of the merging algorithm applied to the segmentation from Fig. 7(b) is shown in Fig. 9. In this example, δ was assigned a value of one centimeter and the algorithm converged after the fifth iteration.

Two features of the algorithm are important for preventing the erroneous merging of catchment basins. The basins formed earliest in the watershed algorithm correspond to the deepest and an attempt to merge them occurs first. In addition, during the merging process, the new catchment basin inherits the maximum depth of the original catchment basins. As seen in Fig. 9(a), regions corresponding to the Sylvian fissure and precentral sulcus have adjacent catchment basins. These sulcal regions should be segmented separately, therefore it is important that their adjacent basins are not merged. The algorithm prevents this as illustrated in Figs. 9(b)-(d) by merging the deepest basins first. An attempt to merge the adjacent basins in the Sylvian and precentral sulcal regions does not occur until each has inherited the maximum depth associated with its respective sulcal region.

The central sulcus, located in the upper center of the images in Fig. 9 is segmented as a single catchment basin after the merging algorithm. However, some sulcal regions are still segmented as several catchment basins. These represent interrupted and pseudo-interrupted sulci [10]. These types of sulci are broken into more than one piece by a gyral ridge and are thus segmented in multiple pieces according to our definition of sulcal regions.

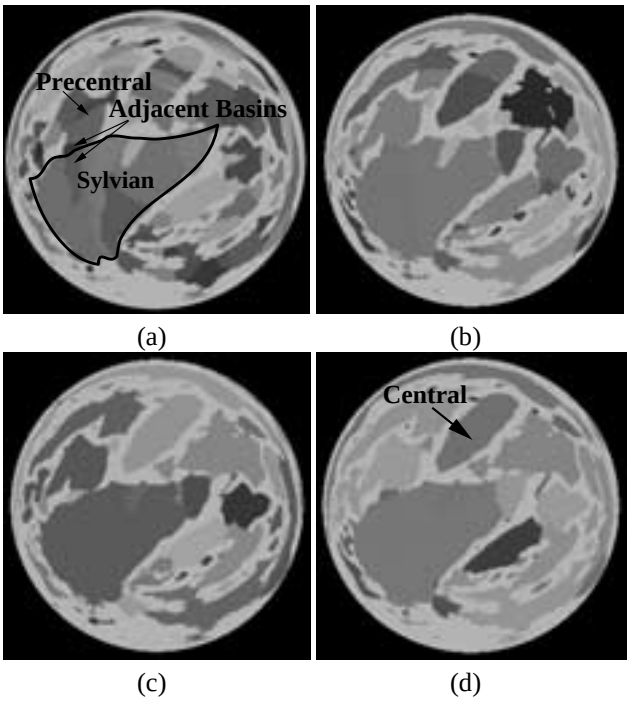

Figure 9. Merging algorithm after (a) iteration 1, (b) iteration 2, (c) iteration 3 and (d) iteration 5.

5. Results

A size filter applied after the merging algorithm to remove small catchment basins gives the final segmentation result shown in Fig. 10. Several sulcal regions have been labeled illustrating that regions corresponding to different sulci are segmented separately. The superior temporal sulcus is an example of an interrupted sulcus which is segmented as more than one catchment basin. In Fig. 11, cross sections of the sulcal segments are shown superimposed on the original MR images. In these images, all sulcal regions have been outlined in white illustrating that the segmented sulcal regions follow the deep folds of the cortical surface. These images do not illustrate that separate regions are segmented for each sulcus, but this has been shown in Fig 10. The segmentation has been applied to fifteen subjects from the Baltimore Longitudinal Study on Aging [13], with accurate and robust results across the various data sets. Sulcal segmentations from four other subjects are displayed on their corresponding spherical maps in Fig 12.

0-7695-0737-9/00 $10.00 (c) 2000 IEEE

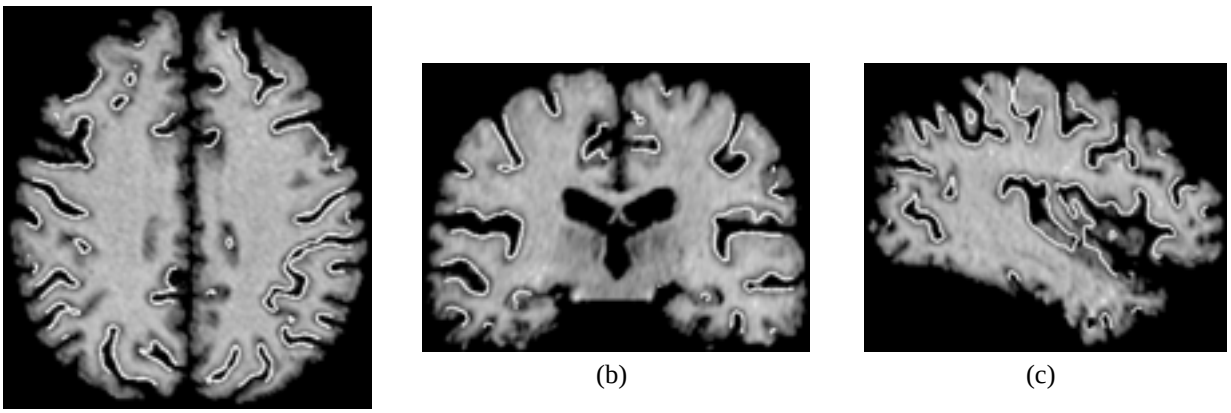

(a) (b) (c)

Figure 11. Cross-sections of sulcal regions superimposed on the original (a) axial, (b) coronal and (c) sagittal MR images.

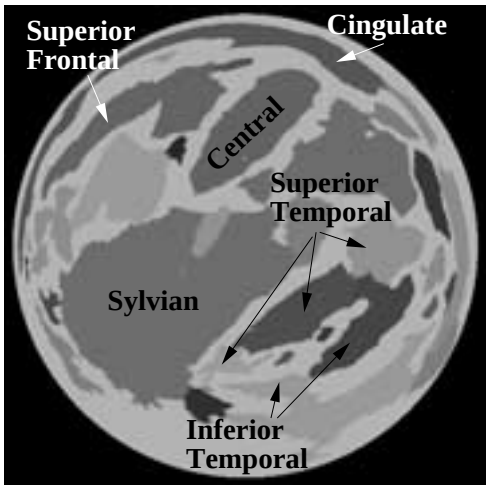

Figure 10. Final sulcal segmentation displayed on the lateral view of the spherical map.

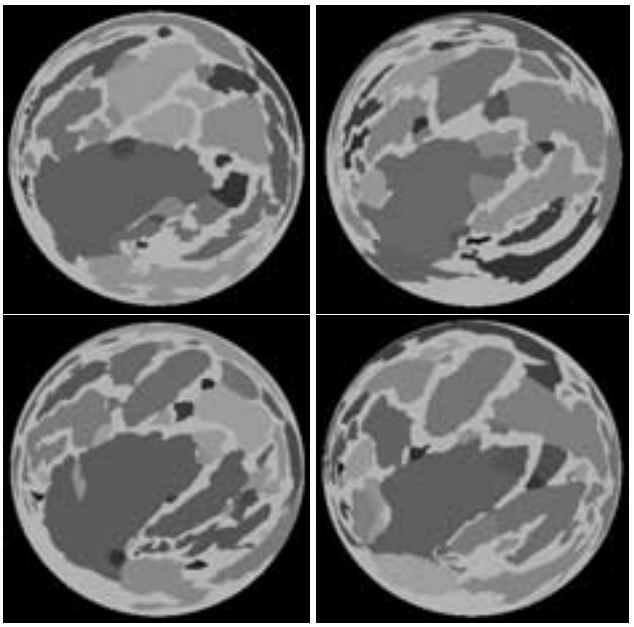

Figure 12. Final segmentation results displayed on the lateral view of spherical maps from four subjects.

6. Discussion

The current segmentation method offers several important improvements over our previous method. In our previous method, the segmentation was based solely on a Euclidean distance transform from the cortical surface to the outer shrink-wrap surface. The Euclidean distance transform can give a rough estimate of cortical depth, but in order to get a true depth measurement, the measurement must be made along the cortical surface. This becomes especially important in highly convoluted regions of the cortex such as the Sylvian fissure. In this region, the cortical surface may curve in a way such that the closest point to the shrink-wrap measured in Euclidean distance could be quite close and the depth measurement will be underestimated.

In our previous method, an initial depth was required to begin the segmentation algorithm. This initial depth needed to be large enough so that distinct sulcal regions were not erroneously joined yet small enough to avoid oversegmentation. The choice of the initial depth threshold greatly affected the results of the final segmentation. In our new method, the segmentation begins at the deepest region of

the cortex removing the need for an initial threshold value. Oversegmentation does occur, but is remedied using a post-processing catchment basin joining algorithm.

Finally, our previous method did not provide a complete parcellation of the sulcal regions. Bridge regions, similar in concept to watershed lines, were used to keep distinct sulcal regions separate. In certain cases, the bridge regions could become thick, resulting in areas within the sulcal regions being labeled as bridge regions. The current method eliminates these "separators", providing a complete parcellation of the sulcal regions.

7. Conclusions and future work

In this paper, we introduced a new method for sulcal segmentation that applies the watershed algorithm to a geodesic distance transform on a cortical surface mesh. The watershed creates an oversegmentation of the sulcal regions which was addressed with a method for merging catchment basins. The merging algorithm presented is one of many reasonable solutions, we are currently investigating other techniques. The next phase of this work is the automated labeling of the sulcal regions according to their corresponding sulcus. We are currently working towards automated labeling based on geometric features of the segmented sulcal regions.

Acknowledgments

The authors would like to thank Chenyang Xu for providing use of the mesh library, various software and many valuable discussions. The authors would also like to thank Sinan Batman for several insightful ideas during the development of this work.

References

[1] A. M. Dale, B. Fischl, and M. I. Sereno. Cortical surface-based analysis I. Segmentation and surface reconstruction. *Neuroimage*, 9:179–194, 1999.

[2] C. Davatzikos and R. N. Bryan. Using a deformable surface model to obtain a shape representation of the cortex. *IEEE Trans. Med. Imag.*, 15:785–795, Dec. 1996.

[3] H. Drury, D. V. Essen, C. Anderson, C. Lee, T. Coogan, and J. Lewis. Computerized mappings of the cerebral cortex: A multiresolution flattening method and a surface-based coordinate system. *J. Cogn. Neuro.*, 8(1):1–28, 1996.

[4] G. L. Goualher, C. Barillot, and Y. Bizais. Modeling cortical sulci with active ribbons. *IJPRAI*, 11(8):1295–1315, 1997.

[5] R. Kimmel and J. Sethian. Computing geodesic paths on manifolds. *Proc. Natl. Acad. Sci.*, 95:8431–8435, 1998.

[6] G. Lohmann and D. Y. von Cramon. Sulcal basins and sulcal strings as new concepts for describing the human cortical topography. In *IEEE Workshop on Biomedical Image Analysis*, pages 24–33, 1998.

[7] G. Lohmann and D. Y. von Cramon. Automatic labelling of the human cortical surface using sulcal basins. In *Medical Image Analysis*, to appear.

[8] D. MacDonald, D. Avis, and A. C. Evans. Multiple surface identification and matching in magnetic resonance images. In *SPIE Proc. VBC '94*, volume 2359, pages 160–169, 1994.

[9] J. Mangin, V. Frouin, I. Bloch, J. Regis, and J. Lopez-Krahe. From 3D magnetic resonance images to structural representations of the cortex topography using topology preserving deformations. *Math. Imag. and Vision.*, 5:297–318, 1995.

[10] M. Ono, S. Kubick, and C. D. Abernathey. *Atlas of the cerebral sulci*. Thieme, New York, 1990.

[11] M. E. Rettmann, C. Xu, D. L. Pham, and J. L. Prince. Automated segmentation of sulcal regions. In *Proc. of Medical Image Computing and Computer-Assisted Intervention (MICCAI)*, pages 158–167. Springer-Verlag, 1999.

[12] S. Sandor and R. Leahy. Surface-based labeling of cortical anatomy using a deformable atlas. *IEEE Trans. Med. Imag.*, 16(1):41–54, 1997.

[13] N. W. Shock, R. C. Greulich, R. Andres, D. Arenberg, P. T. Costa Jr., E. Lakatta, and J. D. Tobin. Normal human aging: The Baltimore longitudinal study of aging. U.S. Government Printing Office, Washington, D.C., 1984.

[14] P. M. Thompson, C. Schwartz, and A. W. Toga. High-resolution random mesh algorithms for creating a probabilistic 3D surface atlas of the human brain. *Neuroimage*, 3:19–34, 1996.

[15] M. Vaillant and C. Davatzikos. Finding parametric representations of the cortical sulci using an active contour model. *Medical Image Analysis*, 1(4):295–315, 1997.

[16] L. Vincent and P. Soille. Watersheds in digital spaces: An efficient algorithm based on emersion simulations. *IEEE Trans. on Pattern Anal. Machine Intell.*, 13(6):583–598, 1991.

[17] C. Xu, D. L. Pham, J. L. Prince, M. E. Etemad, and D. N. Yu. Reconstruction of the central layer of the human cerebral cortex from MR images. In *Proc. of Medical Image Computing and Computer-Assisted Intervention (MICCAI)*, pages 481–488. Springer-Verlag, 1998.

[18] C. Xu, D. L. Pham, M. E. Rettmann, D. N. Yu, and J. L. Prince. Reconstruction of the human cerebral cortex from magnetic resonance images. *IEEE Trans. Med. Imag.*, 18(6):467–480, 1999.

[19] X. Zeng, L. H. Staib, R. T. Schultz, H. Tagare, L. Win, and J. S. Duncan. A new approach to 3D sulcal ribbon finding from MR images. In *Proc. of Medical Image Computing and Computer-Assisted Intervention (MICCAI)*, pages 148–157. Springer-Verlag, 1999.

0-7695-0737-9/00 $10.00 (c) 2000 IEEE